DOI 10.4430/bgo00414

Present-day seismicity of the Matese Massif (central-southern Apennines, Italy): new constraints on the seismotectonic setting of the central and southern sides

G. Milano

Istituto Nazionale di Geofisica e Vulcanologia, Osservatorio Vesuviano, Napoli, Italy

(Received: 27 October 2022; accepted: 4 February 2023; published online: 13 April 2023)

ABSTRACT We investigated the 2009-2020 instrumental seismicity of the Matese Massif. With the exception of two relevant seismic sequences (2013-2014 and 2016-2017, M_{MAX} = 4.9), the background seismicity consists of low magnitude seismic swarms (M_{MAX} = 3.3) located at the borders of the massif, and sparse single events (M_{MAX} = 3.5). The focal mechanisms of the single events located near the NW and west edges of the massif suggest that this seismicity occurs on SW dipping, ca. NW-SE striking normal fault segments, in accordance with the kinematics of the Aquae Iuliae Fault. The focal mechanisms of two low magnitude seismic swarms located in the morphological depression, separating the Matese Massif from the Sannio Mountains, provide seismological evidence, never previously observed in this area, of the existence of an active east-western fault segment with dextral strike-slip kinematics. To the west of this area, there is no seismological evidence of strike-slip kinematics, whereas such evidence is found to the east. This area could represent the westernmost expression of the active strike-slip regime that characterises the Apulian foreland. Along the faults situated on the southern side, the very rare detected seismicity could be related to the high emission of CO_2-bearing gas vents located near these faults. Considering the time elapsed from the last destructive earthquake (1349), the possible sources of the poorly known 346 and 1293 earthquakes, and the rare seismicity detected in the last 25 years, we speculate that the south-western side of the Matese may be affected by large earthquakes in the future.

Key words: seismotectonics, Matese Massif, seismic swarm, fault-plane solution, Apulian foreland.

1. Introduction

The studies on the background seismicity, consisting of low-magnitude events and low-magnitude seismic sequences and swarms, can provide useful information to deepen the seismotectonic knowledge of an area. These studies allow the identification and geometry of small active fault segments, as well as their kinematics, and can provide useful information on the present-day stress field. The analysis of the background seismicity is of particular relevance for areas, such as the Sannio-Matese, hit by large historical earthquakes interspersed with long periods of quiescence.

The Sannio-Matese area is a region that marks the transition between the central and southern Apennines (Fig. 1) and it is one of the areas of the Italian peninsula with the highest seismogenic potential (e.g. Chiarabba and Amato, 1997; Improta *et al.*, 2000). Large historical destructive

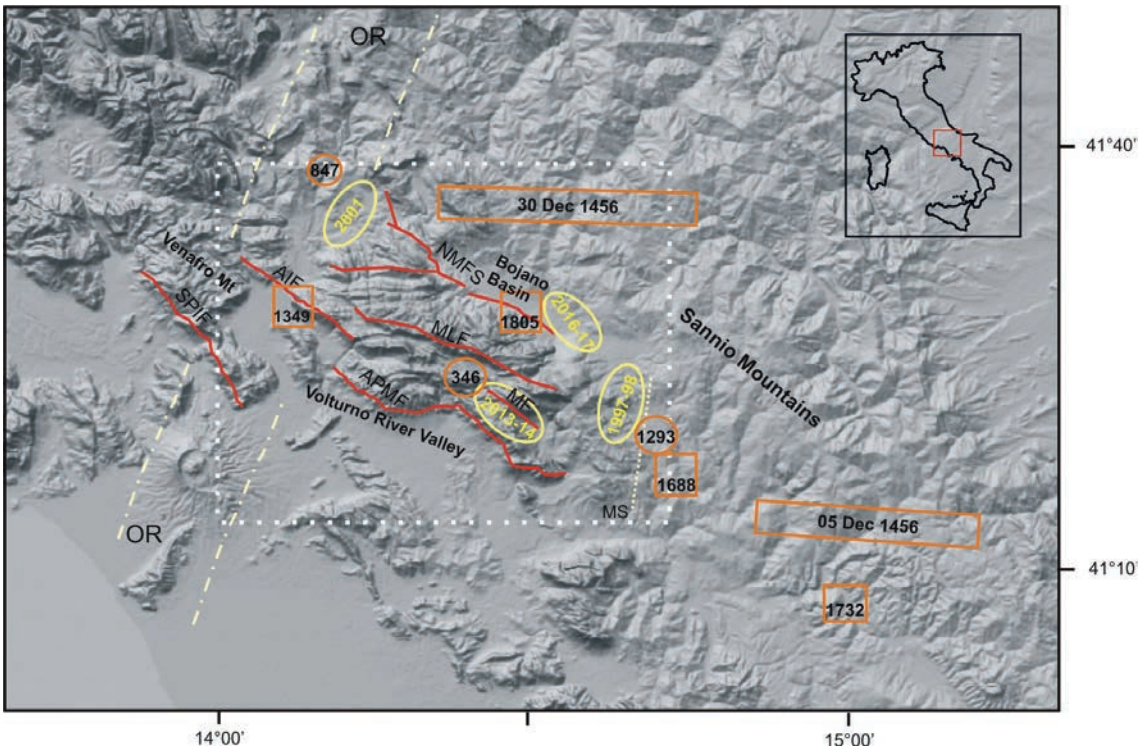

Fig. 1 - Map showing the Sannio-Matese area. The area limited by the white dashed line encloses the Matese Massif. The main Quaternary faults (red lines) are from: SPIF - San Pietro Infine Fault (Boncio *et al.*, 2016); APMF - Ailano Piedimonte Matese Fault (Boncio *et al.*, 2016); MLF - Matese Lake Fault (Boncio *et al.*, 2016); AIF - Aquae Iuliae Fault (Galli and Naso, 2009); NMFS - North Matese Fault System (Galli and Galadini, 2003; Galli and Naso, 2009). MF represents the fault segment for the 2013-2014 sequence (Ferranti *et al.*, 2015). OR, enclosed between two light yellow lines dashed with dots and dash, represents the Ortona-Roccamonfina structural lineament. The small dotted light yellow line MS is representative of the morphological depression that divides the Matese Massif from the Sannio Mountains. The squares with the dates represent the epicentres of the main historical earthquakes that occurred in the Sannio-Matese area (DISS Working Group, 2021), whereas the ellipses with the dates indicate the location of the main seismic sequences since 1995. The circles with the dates represent the epicentres of the 346, 847 (Guidoboni *et al.*, 2007), and 1293 (Rovida *et al.*, 2022) poorly known earthquakes. The rectangles with the dates represent the composite seismogenic sources of the 1456 multiple earthquake (DISS Working Group, 2021).

earthquakes (Fig. 1) with I_o > IX MCS occurred in 1349, 1456, 1688, 1732, and 1805, whereas poorly known earthquakes struck the area in 346, 847, and 1293 (e.g. Di Bucci *et al.*, 2005b; Fracassi and Valensise, 2007; Rovida *et al.*, 2022). The 1349 and 1805 earthquakes had their epicentre in the Matese Massif (hereafter MM) and affected the southern and the northern sides, respectively. Compared to the fairly well-documented 1805 earthquake, the 1349 earthquake, due to its age, has no detailed historical documentation. This earthquake includes at least three main shocks, all probably occurring on 9 September. Geological investigations, augmented by geomorphological and historical analyses, have suggested a SW dipping, NW-SE striking normal fault, located on the SW side of the MM, as responsible for the southernmost shock of the 1349 earthquake (Galli and Naso, 2009). Boncio *et al.* (2016, 2022) suggested that also the poorly known 349 and 1293 earthquakes (Fig. 1) could be located along the southern side of the MM.

The instrumental seismicity of the MM showed sparse low-magnitude single shocks (M < 2.0) and low magnitude seismic sequences (M_L < 4.2) at its edges (Milano *et al.*, 2008). Between late 2013 and early 2014, a significant seismic sequence, following an M_W = 4.9 event,

struck the internal south-eastern sector of the MM. Following this sequence, interest in the MM, in particular on the less known southern side, has considerably increased. Geological studies (Boncio *et al.*, 2016, 2022) have provided new constraints on the fault systems located along the western and southern sides. However, the degree of knowledge of the single fault segments in terms of their exact positioning and extension in depth, geometry, and kinematics, is still a matter of research. There are a number of questions on the southern side of the MM: which fault segments are still active along the southern side? Are the active fault segments, if any, capable of generating an $M > 6.0$ event? What is the relation, if any, between the occurrence of low-magnitude seismic sequences and swarms occurring at the edges of the MM and the regional tectonics?

Here, we investigate the present-day background seismicity of the MM in order to provide a contribution on the seismotectonic setting of the southern side. The study area takes into consideration the location of the 1349 Aquae Iuliae Fault [AIF; Galli and Naso (2009)], **t**o the west, and the morphological depression separating the MM from the Sannio Mountains to the east. The analysed seismicity is that which occurred between the years 2009 and 2020. In this interval, in addition to the 2013-2014 seismic sequence, low-magnitude seismic swarms occurred near the NW tip of the 1349 seismogenic source and near the south-eastern edge of the MM.

A manual re-picking of P and S phases has been performed on the collected waveforms of the seismic events occurring in the area. The revision also enabled compiling a P-wave polarity data set to compute well-constrained fault-plane solutions. The results of this study, also discussed in light of the recent geological and geophysical results and with previous seismological data, add new original information both on the southern side and on the NW and SE edges of the MM.

2. Tectonic overview and seismicity of the area

The Matese is a massif of carbonate rocks characterised by the highest prominent topographic (maximum elevation of about 2000 m a.s.l.) of the Sannio-Matese area. The MM, WNW-ESE trending, is about 50 km long and 20 km wide, and extends between the depression of the middle Volturno River valley to the west and SW, and the Bojano basin to the north (Fig. 1). To the east, a morphological depression, N-S to NNW-SSE striking, divides the MM from the Sannio Mountains. The upper and middle Volturno River valley lies inside the NNE-SSW striking Ortona-Roccamonfina structural lineament.

The morphology of the MM is the result of the Quaternary activity on the NW-SE striking extensional faults, which overlapped the previous transpressional deformation (Ferranti, 1997; Calabrò *et al.*, 2003). This motion formed a horst bordered by NE dipping and SW dipping normal faults (Boncio *et al.*, 2016). The NE dipping North Matese Fault System [NMFS in Fig. 1; Galli *et al.* (2002) and Porfido *et al.* (2002)] forms the northern border of the MM (Di Bucci *et al.*, 2005b) and crosses the Bojano lacustrine basin. This complex normal fault system is responsible for one of the likely main-shocks of the 1456 seismic sequence and for the 1805 earthquake, both with $M_w > 6.5$ (DISS Working Group, 2021). On the south-western side of the MM, the AIF (Fig. 1) is considered the source of large historical and prehistorical earthquakes, including the 9 September 1349 event, $M_w = 6.6$, (Galli and Naso, 2009). Along the southern side of the MM is located the SW dipping Ailano Piedimonte Matese normal fault (APMF in Fig. 1), which extends westwards and uplifts the range relative to the Volturno basin (Boncio *et al.*, 2016). The inner sector of the MM is dissected by the SW dipping Matese Lake Fault, which borders the northern side of a linear, >30-km long asymmetric basin (MLF in Fig. 1). East of the MM is the seismogenic

source of the M_W = 7.0, 1688 earthquake [Fig. 1; see DISS Working Group (2021)], although its exact location and direction is still under study [see discussion in Di Bucci *et al.* (2005a)].

An extension rate of about 4-5 mm/yr characterises the sector of the Apennine chain that includes the MM, suggesting a partitioning of deformation due to different seismogenic structures (Giuliani *et al.*, 2009; Boncio *et al.*, 2016; Cowie *et al*., 2017). Esposito *et al.* (2020) have shown that no significant GPS deformation is detected in the inner fault system of the MM.

No strong earthquake (M > 6.0) has been associated with the aforementioned faults since the 1805 earthquake. Over the past three decades before the year 2013, the instrumental background seismicity of the MM was characterised by a few single events (M_{Lmax} ~2.5) and by low magnitude seismic sequences and swarms. Two significant seismic sequences, which lasted several months and consisted of thousands of events (Milano *et al.*, 2002, 2005), occurred in the south-eastern (1997-1998, M_{Lmax} = 4.2) and in the north-western (1997-1998, M_{Lmax} = 3.6) edges of the MM (see Fig. 1 for the location of these seismic sequences). The hypocentres of this seismicity lie prevalently within 15 km of the crust. A relevant seismic sequence occurred between late 2013 and early 2014 following an M_W = 4.9 event. This sequence struck the internal SE of the MM and the hypocentres, contrary to what was previously observed on the depth of the seismicity of the area, confined between 10 and 20 km in depth. The focal mechanisms of the most energetic events of this sequence suggest that the seismicity occurred on a SW dipping, NW-SE striking, 10-km long normal fault, near parallel to the normal faults mapped at the surface [Ferranti *et al.* (2015), see also Milano (2014), Di Luccio *et al.* (2018), and Trionfera *et al.* (2020) for the different interpretation of this sequence]. Noteworthy are also the 2016 and 2017 seismic activities that occurred in the Bojano basin (Fig. 1). The 2016 episode was characterised by an M_W = 4.3 main event that occurred after a significant increment of the seismicity, in particular, in the 36 hours leading up to the main event. The roughly NNW-SSE distribution of the seismicity, the depth of the events, and the focal mechanisms were compatible with the NE dipping, NW-SE striking, 1805 seismogenic source [see Milano (2016), Moretti *et al.* (2017), and Trionfera *et al.* (2020), for details].

3. Data and earthquake locations

The study area extends and includes the seismogenic source of the 1349 earthquake, to the western and south-eastern edge of the MM. We used seismic data recorded by the RSN (Rete Sismica Nazionale) operated by INGV (Istituto Nazionale di Geofisica e Vulcanologia, doi: 10.13127/sd/x0fxnh7qfy). The configuration of this seismic network, consisting of more than 500 stations, ensures a fairly good azimuthal coverage of the Italian territory and allows locating low magnitude events (M_L ~2.0). We also used seismic data recorded by temporary seismic stations installed in the study area following the occurrence of relevant seismic activity [e.g. 2016 sequence: Moretti *et al.* (2017)]. The data recorded by a test seismic station installed in 2018 in the upper Volturno Valley, as part of a pre-agreement with local administrations for environmental monitoring, has also been used. The digital waveforms of the seismic events, which occurred in the study area and related to the 2009-2020 time interval, have been collected and analysed. The visual inspections of the seismograms were carried out to perform a manual re-picking of the P- and S-wave arrivals in order to correct any misinterpretation present in the catalogue, in particular, on S phase for the reliability of the focal depth.

Following the approach we used in previous studies on the seismicity of the Sannio-Matese area (e.g. Milano *et al.*, 2008), we selected the seismic events recorded by a minimum of five stations and with at least five P- and four S-phase readings. We performed several trials to

evaluate the reliability of the earthquake location taking into account the velocity model and the azimuthal coverage of the seismic stations in the area. Considering the quite good azimuthal coverage of the seismic stations in the study area (Fig. 2), we performed several location trials on events with variable numbers of recordings. These trials led to estimating the dependence of earthquake location from the velocity model, using the few available for the area, and reported in previous papers (Chiarabba and Amato, 1997; Iannaccone *et al.*, 1998; Milano *et al.*, 1999; Improta *et al.*, 2000; Frepoli *et al.*, 2017). The trials showed no significant differences among the earthquake location parameters if only data of the seismic stations within a radius of ~50 km are utilised. On the contrary, if also data of the seismic stations more than 50 km away from the epicentral area are utilised, the velocity model reported in Milano *et al.* (1999) shows the highest stability of earthquake location parameters because it minimises both the root mean square (RMS) error on the arrival times and the location errors. This velocity model is also defined at larger depths as compared to other models. Therefore, we adopt the above velocity model (Table 1), already used in previous studies on the seismicity of the area. We used the HYPOINVERSE-2000 code (Klein, 2002) to locate the earthquakes. After several trials, the DIS parameter, which controls the distance weighting, has been set in order to exclude, in the interactive earthquake processing, the P and S phases recorded at the seismic stations located more than 80 km away from the epicentres. We used the value of 1.78 for the *Vp/Vs* ratio, obtained by the trial-and-error procedure. The utilised parameters lead to obtain error locations less than 1.5 and 2.2 km for the horizontal position and depth, respectively; the RMS values are less than 0.45 s. More in particular, about 82% of the relocated seismicity has horizontal errors less than 1.0 km, 61% has vertical errors less than 1.5 km, and 60% has RMS values less than 0.3 s.

About 43% of seismicity was re-located with a number of P and S phases greater than 15, whereas about 18% with at least five P and four S phases. We computed fault-plane solutions by means of the FPFIT grid-search algorithm (Reasenberg and Opphenheimer, 1985). The number of polarity used (>10) and the good azimuthal coverage of the seismic stations at short epicentral distances (<50 km) lead to stable solutions, with average errors on the maximum likelihood solutions <10 for strike, dip and rake. Table 2 reports the focal mechanism data of the single events and also includes the localisation errors for each event.

Table 1 - 1D velocity model used for locating earthquakes.

Vp	**Depth**
4.5	0.0
5.5	2.0
5.8	10.0
6.7	23.0
8.2	35.0
8.3	50.0

4. Seismological results

The epicentral distribution and the hypocentral distributions of more than 750 relocated events occurred between 2009 and 2020, with the exception of the events of the 2013-2014 sequence and the 2016 and 2017 sequences in the Bojano basin, are shown in Fig. 2. Many of the events are located west of the San Pietro Infine Fault (SPIF), therefore outside of the study area,

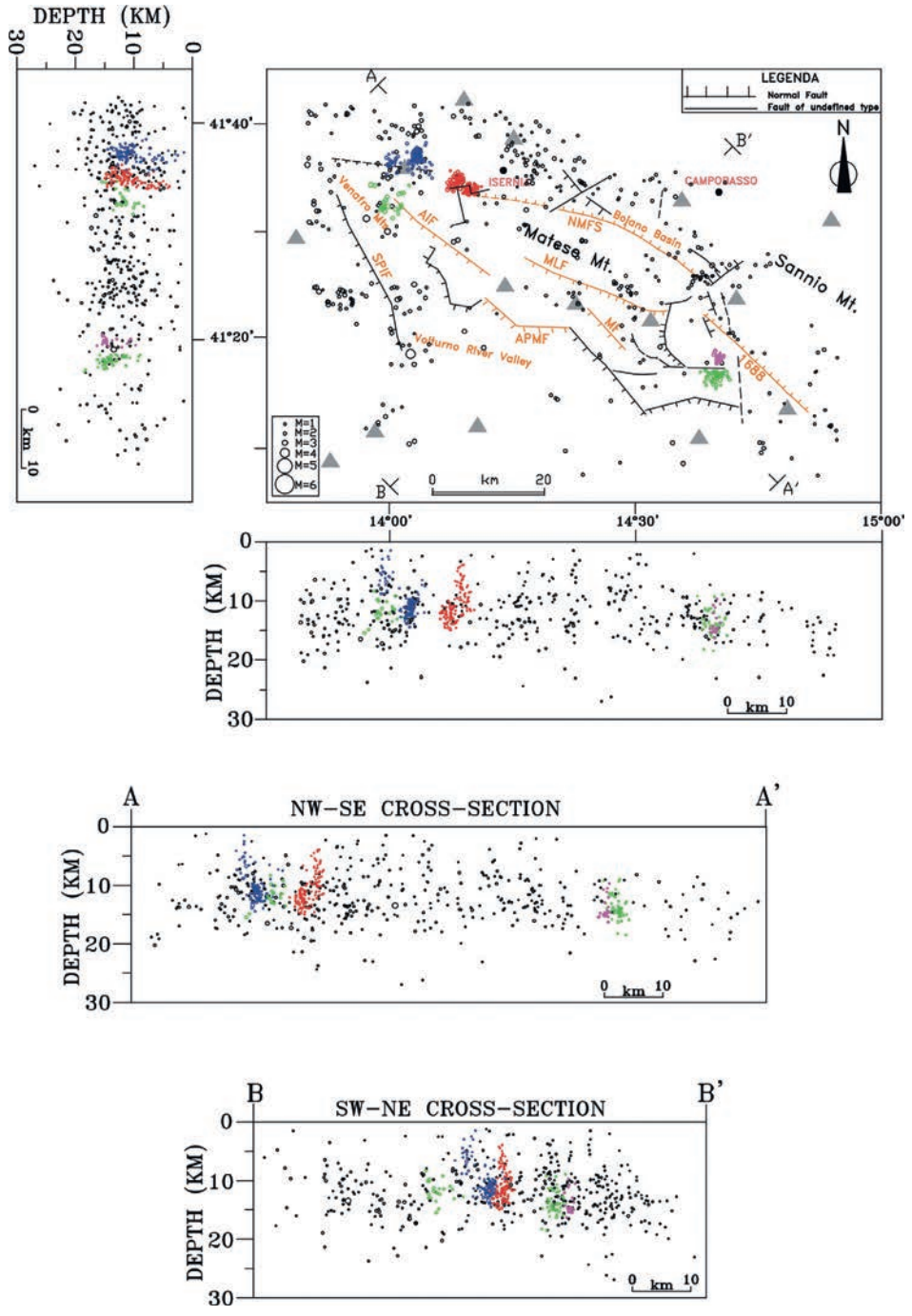

Fig. 2 - Map showing the main structural lineaments of the Matese area (redrawn after CNR-PFG, 1983) on which is reported the epicentral distribution of the relocated seismicity and N-S, W-E, NW-SE, and NE-SW hypocentral distributions. In yellow are schematically reported the traces of the Quaternary faults shown in Fig. 1. The trace of the fault of the 1688 earthquake is also reported (DISS Working Group, 2021). MF is representative of the 10-km long, SW-deepening normal fault proposed by Ferranti *et al.* (2015) as the source of the 2013-2014 sequence. The dark grey triangles are the permanent seismic stations running in the area. Black circles represent the single events; red circles, green circles, and blue circles denote the events of the 2010, 2011, and 2020 seismic swarms, respectively, occurred in the north-western edge of the MM; green circles and magenta circles denote the events of 2014 and 2018 seismic swarms, respectively, occurred in the south-eastern edge of the MM.

belong to low-magnitude seismic sequences that occurred in August 2009 and between February and April 2013 (see Frepoli *et al.*, 2017). The relocated seismicity consists in single events and low-magnitude seismic swarms. The single events ($1.6 \leq M_L \leq 3.7$) occurred sparsely in the study area and showed no evidence of any preferred alignments. A few events are located in the inner part of the MM and along its southern side; the magnitude of these events is less than 2.0. The hypocentres are mainly at depths between 5 and 16 km (cross-sections in Fig. 2). The most energetic events (four events with $3.0 \leq M_L \leq 3.7$) are located between the Venafro Mountains and the middle Volturno Valley. The fault-plane solutions of these events and those of two events with M_L ~2.0 located near the NW tip of the AIF show kinematics compatible with normal dip-slip faults with limited strike-slip component (Fig. 3). Common elements of these focal mechanisms are NW dipping, NW-SE to NNW-SSE striking planes. The surface projection of the sub-horizontal T-axes of these focal mechanisms are roughly aligned along the NE-SW direction (Fig. 3). The fault-plane solutions of two events with M_L ~2.5 located near the south-eastern edge of the MM, at a depth of about 15 km, show different kinematics: normal dip-slip solution, with NW-SE striking nodal planes, and strike-slip solution, with about N-S and E-W striking nodal planes. The surface projection of the T-axes of these focal mechanisms aligned along the NE-SW direction.

Low magnitude seismic swarms occurred in 2010, 2011, 2014, 2018, and 2020. The first two and the last one were located between the NW tip of the AIF, the Venafro Mountains and the NW tip of the NMFS, whereas the 2014 and 2018 swarms were located near the south-eastern edge of the MM. The main results for each swarm are reported below.

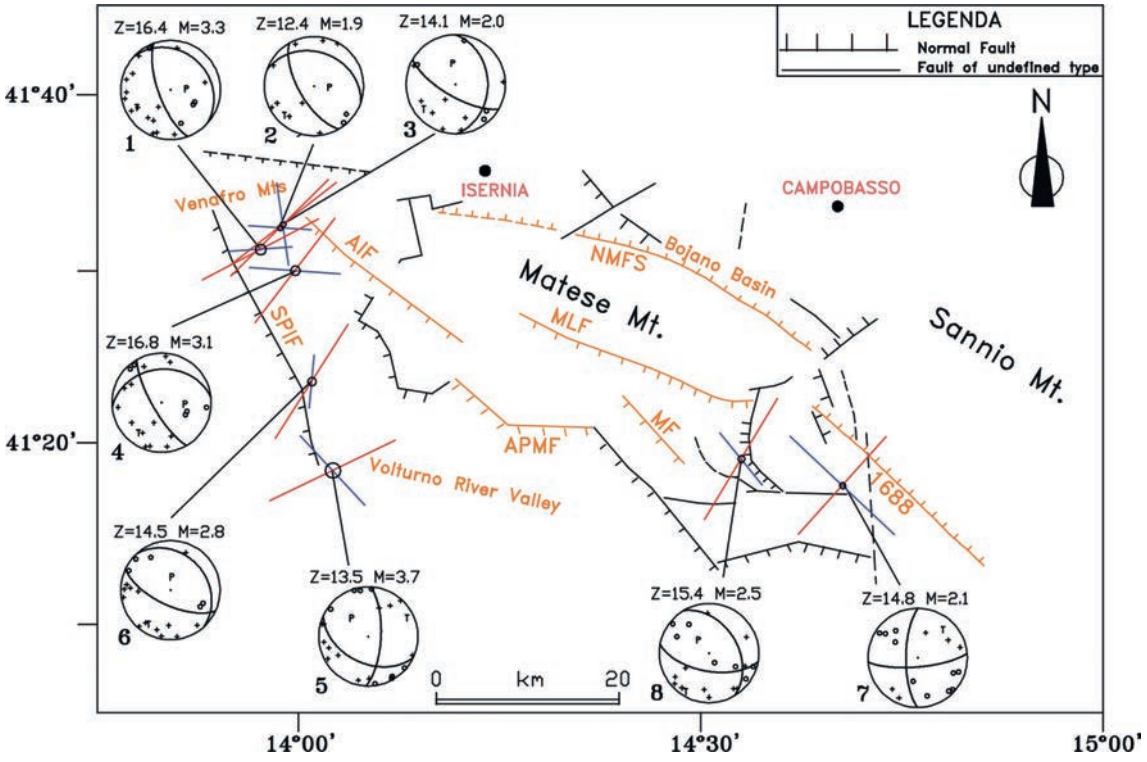

Fig. 3 - Fault-plane solutions of the single events occurred in the study area. The focal mechanisms report the depth and magnitude of the events, and an identification number (ID in Table 2). The surface projection of the T- (red) and P- (blue) axes of each focal mechanism is reported at the epicentre. The length of each axis is proportional to the cosine of the plunge (see Table 2 for further information).

Table 2 - Focal mechanisms data relating to single events. For each event, the date and origin time, latitude (Lat N), longitude (Long E), hypocentral depth (Depth), magnitude (Mag), number of P and S phases (No), maximum azimuthal gap between seismic stations (Gap), root mean square (RMS), maximum error on horizontal (EH) and depth (EZ) are reported; as well as the strike, dip, and slip of focal plane A (STR-A, DIP-A, SLIP-A) and plane B (STR-B, DIP-B, SLIP-B); the azimuth and plunge of P- (Az-P, Plg-P) and T-axes (Az-T, Plg-T), respectively.

ID	Date	Origin Time	Lat N	Long E	Depth	Mag	No	Gap	RMS	EH	EZ	STR-A	DIP-A	SLIP-A	STR-B	DIP-B	SLIP-B	Az-P	Plg-P	Az-T	Plg-T
1	20130414	022036.30	41-31.19	13-57.19	16.40	3.30	29	111	0.42	0.7	1.3	160.0	70.0	- 80.0	- 47.3	22.3	- 115.5	86.1	63.7	242.3	24.5
2	20130417	001616.31	41-32.41	13-58.64	12.40	1.90	18	121	0.27	0.5	1.2	150.0	65.0	- 70.0	- 70.7	31.6	- 126.3	93.8	64.3	225.3	17.7
3	20130418	044116.44	41-32.61	13-58.85	14.10	2.00	19	76	0.29	0.6	1.3	120.0	70.0	- 120.0	- 0.6	35.5	- 36.1	352.2	54.8	232.1	19.5
4	20130708	092802.06	41-29.99	13-59.77	16.80	3.10	29	83	0.39	0.7	1.6	150.0	75.0	- 60.0	264.2	33.2	- 151.8	93.9	50.7	217.2	24.1
5	20160628	023342.82	41-18.69	14-02.58	13.50	3.70	27	71	0.36	0.5	1.7	115.0	45.0	- 150.0	2.7	69.3	- 49.1	317.2	48.6	64.2	14.5
6	20170930	235811.25	41-23.72	14-01.01	14.50	2.80	30	99	0.28	0.4	1.3	115.0	65.0	- 100.0	- 42.4	26.8	- 69.6	5.5	68.4	212.5	19.4
7	20200817	200355.71	41-17.84	14-40.59	14.80	2.10	24	68	0.32	0.6	1.1	85.0	75.0	160.0	180.4	70.7	15.9	133.3	2.9	41.9	24.6
8	20201101	160829.92	41-19.34	14-33.04	15.40	2.50	27	70	0.33	0.6	0.9	100.0	60.0	- 120.0	- 30.9	41.4	- 49.1	320.9	62.1	211.1	10.2

4.1. The 2010 swarm

Regarding the swarms located in the NW of the study area, the first (red dots in Fig. 4) occurred at the end of May 2010 and was triggered by an M_L = 3.3 earthquake (29 May, 15:04). About 150 events ($1.0 \leq M_L \leq 2.5$) occurred within the next 48 hours from the main event. The epicentral distribution does not show a clear alignment. The events seem to cluster into two groups: the first approximately along the NE-SW direction and the second approximately along the E-W, respectively. This peculiarity is also evident in the W-E and NW-SE cross-sections. The events belonging to the first group have depths between 10 and 15 km, whereas those belonging to the second group have depths between 5 and 12 km (cross-sections in Fig. 4). The fault-plane solutions show different kinematics: normal dip-slip with a limited strike-slip component, e.g. the one related to the event that triggered the swarm (No. 1 in Fig. 5), and oblique solution (No. 2 and 3 in Fig. 5). The common element of the normal dip-slip focal mechanisms is the SW dipping, ~NW-SE striking plane. The oblique solutions show striking nodal planes along the WNW-ESE and NNE-SSW directions. The surface projection of the T-axes of the normal dip-slip focal mechanisms aligned along the NNE-SSW direction, whereas those related to the oblique focal mechanisms aligned along the NNW-SSE direction (Fig. 5).

4.2. The 2011 swarm

The second swarm (October 2011; green dots in Fig. 4) was not triggered by a main event. It was constituted by about 25 events between 1-4 and 18-30 October. The events ($1.5 \leq M_L \leq 2.6$) were located close to the NW tip of the AIF and had a focal depth between 9 and 15 km (cross-sections in Fig.4). The focal mechanisms of three events ($2.2 < M_L < 2.6$, depth ~12 km) show strike-slip solutions with the ~NNE-SSW and ~ESE-WNW striking nodal planes. The surface projection of the T- and P-axes aligned along the NE-SW and NW-SE directions, respectively (Fig. 5).

4.3. The 2020 swarm

The 2020 swarm (blue dots in Fig. 4) started with an increase in seismicity, compared to the background one, following an M_L = 1.8 event (8 August). About 25 events, 3 of which with $2.0 \leq M_L \leq 2.7$, occurred until the beginning of September. Starting from 17 September, a notable

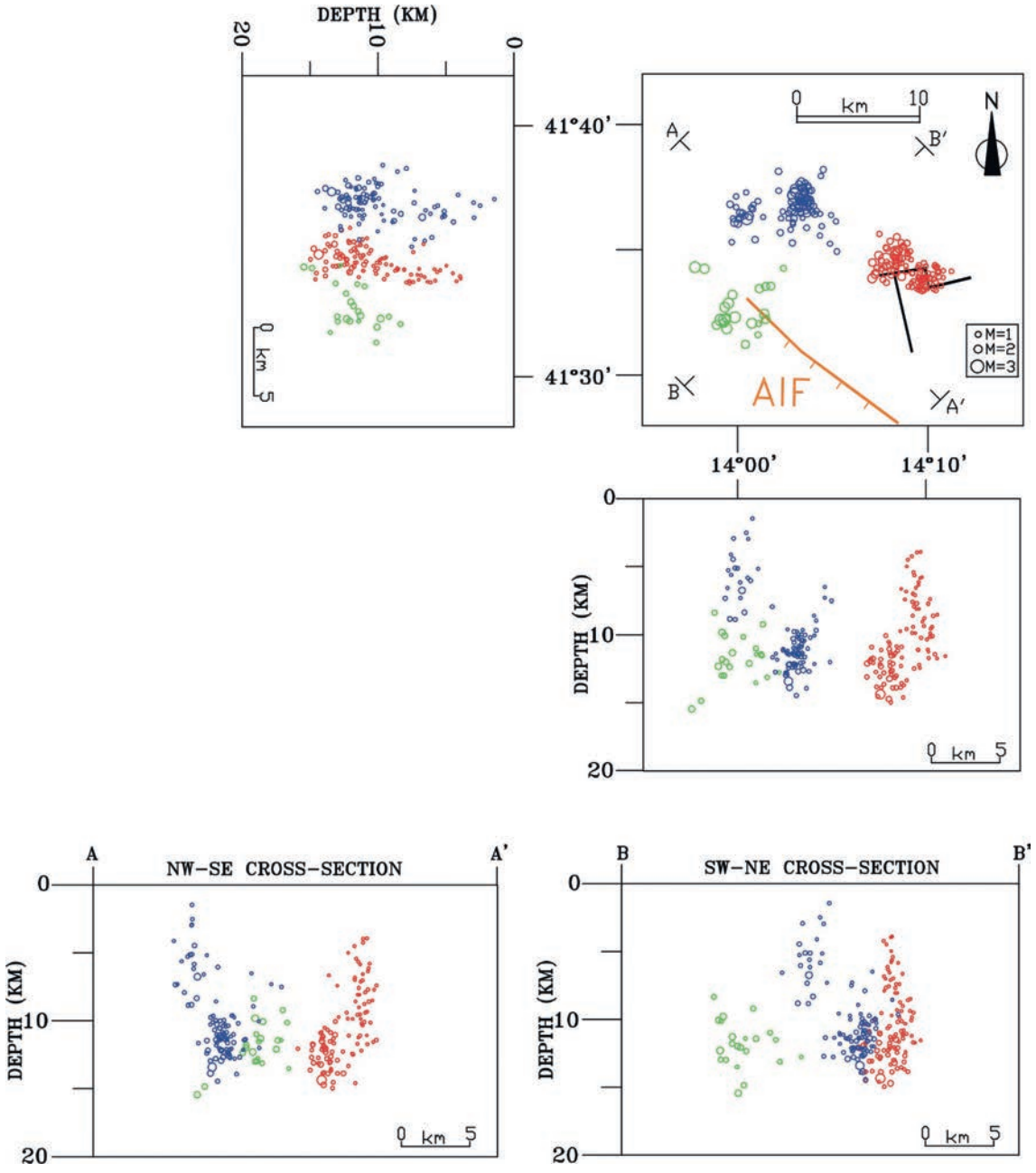

Fig. 4 - Epicentral distribution of the seismic swarms localised between the north-western tip of AIF, the Venafro Mountains, and the north-western tip of NMFS and N-S, W-E, NW-SE, and NE-SW hypocentral distributions. Red circles, green circles, and blue circles denote the events belonging to 2010, 2011, and 2020 seismic swarms, respectively.

increase in seismicity occurred following an M_L = 1.5 event. This swarm, about 100 events almost all of them with M_L < 2.0, lasted until 10 October. Only 12 events had 2.0 ≤ M_L ≤ 2.5 and the most energetic event occurred at the end of the swarm (M_L = 3.1, 13 October, 14:09). After this event, the seismic activity ceased rapidly, only nine events being detected until 10 October. Note that, for the first time in this area, the most energetic event occurred at the end of a swarm. The

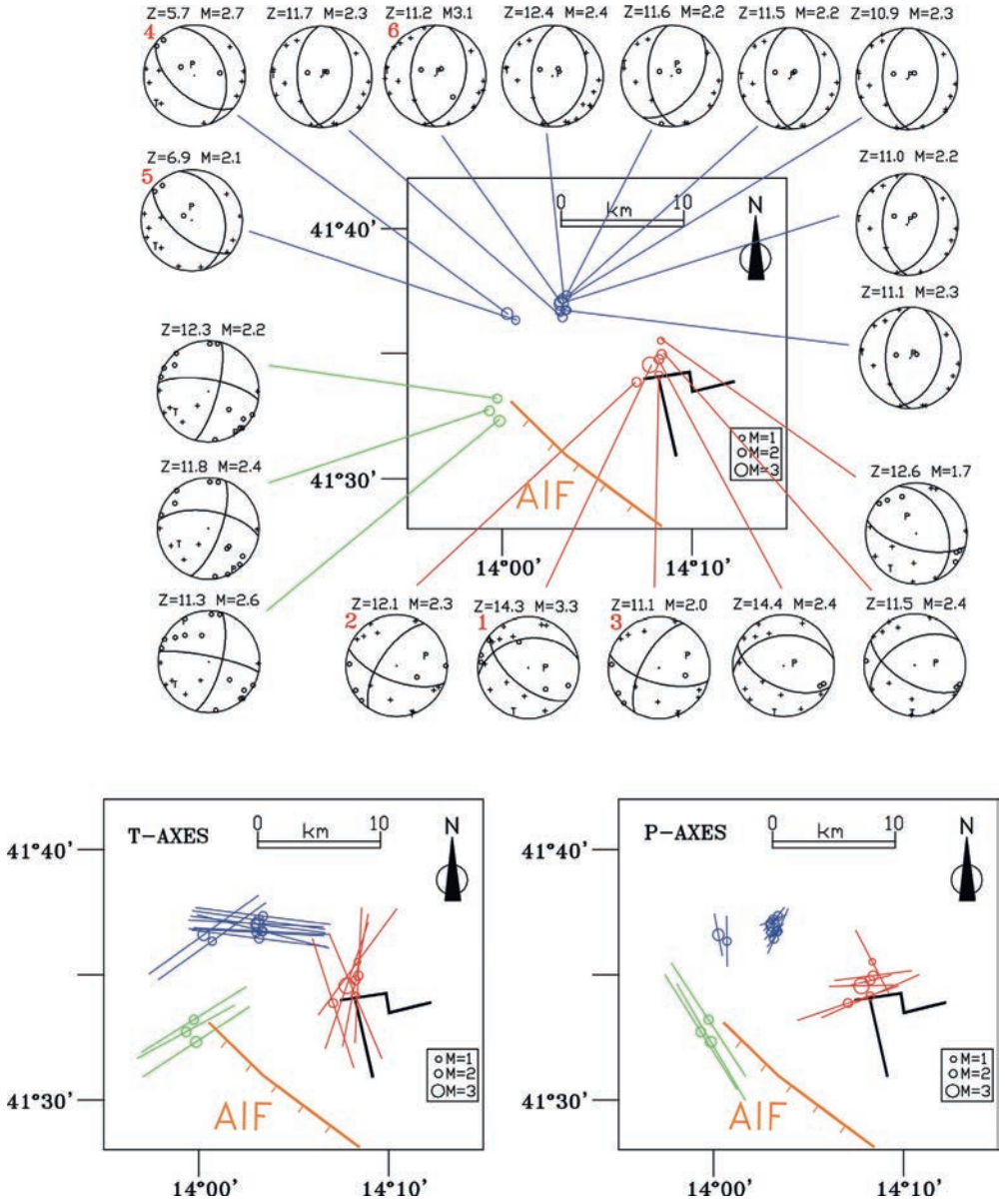

Fig. 5 - Top: fault-plane solutions of the 2010 (red), 2011 (green), and 2020 (blue) seismic swarms, respectively. For each focal mechanism, the depth and the magnitude of the event are reported. Bottom: surface projection of the T- (left) and P- (right) axes of the focal mechanisms. The length of each axis is proportional to the cosine of the plunge.

epicentral distribution shows that the events are concentrated in two different groups (Fig. 4): one group contains the events between August and the beginning of September (westernmost), whereas the second group contains the events starting on 17 September. The events of the first cluster have a depth between 3 and 8 km, while the events of the second cluster, whose epicentral distribution roughly aligns along the N-S direction, have a depth between 8 and 13 km (see cross-sections in Fig. 4). The fault-plane solutions of two events of the first cluster show normal dip-slip solutions with ~NNW-SSE striking nodal planes and sub-horizontal T-axes in the ~NE-SW direction (Nos. 4 and 5 in Fig. 5). The focal mechanisms of the events of the second

cluster show normal dip-slip solutions with ~N-S striking nodal planes (e.g. No. 6 in Fig. 5) and sub-horizontal T-axes aligned in the ~E-W direction.

4.4. The 2014 swarm

Regarding the swarms located near the south-eastern edge of the MM, the first one (green dots in Fig. 6) started on 25 September, 2014 with an M_L = 1.6. It lasted about 36 hours and consisted of about 50 events with $1.5 \leq M_L \leq 2.8$. The epicentral distribution shows a rough alignment of the events along the E-W direction; the depth of the events is between 9 and 16 km (cross-sections in Fig. 6). The N-S hypocentral distribution shows a coarse deepening of the seismicity towards south. The focal mechanisms of the events with $M_L > 2.0$ (depth between 14 and 16 km) show strike-slip solutions with roughly N-S and E-W striking nodal planes (Fig. 7). The surface projection of the T- and P- axes aligned along the NE-SW and NW-SE directions, respectively (Fig. 7).

4.5. The 2018 swarms

The 2018 swarm is located about 3 km north of the 2014 swarm (chain dots in Fig. 6). This swarm started with an M_L = 1.8 event on 2 September (09:02). It lasted a few days and consisted of about 25 events with $1.5 \leq M_L \leq 3.1$ (depth between 13 and 15 km; cross-sections in Fig. 6). The most energetic event occurred on 9 September (02:22; depth ~15 km; M_L = 3.1). The focal mechanisms of the events with $M_L > 2.2$ (depth between 14.5 and 15.5 km) show strike-slip solutions with about N-S and E-W striking planes (Fig. 7). The surface projection of the T- and P- axes aligned along the NE-SW and NW-SE directions, respectively (Fig. 7).

5. Discussion

5.1. Seismicity in the western and north-western edges

The normal dip-slip kinematics of the focal mechanisms of the single events located between the Venafro Mountains and middle Volturno Valley suggests that this seismicity is related to the large-scale present-day extensional strain field that affects the Apennine chain. Considering that the common element of these focal mechanisms is a ~SW dipping, NW-SE to NNW-SSE striking plane, we maintain that the detected seismicity occurred prevalently on SW dipping, NW-SE striking normal fault segments. This pattern is in accordance with the kinematics of the normal faults mapped at the surface along the south-western side of the MM (Galli and Naso, 2009; Boncio *et al.*, 2016). The strike-slip kinematics of the focal mechanisms of the swarm occurring near the NW tip of the AIF in 2011 does not match with the kinematics of this fault. However, the NE-SW striking T-axes of the focal mechanisms suggest that the events of this swarm were also due to the NE-SW extension of the Apennine chain.

Different patterns show the 2010 and 2020 seismic swarms. The focal mechanisms of the 2010 swarm show both normal dip-slip and oblique solutions. The orientation of the T-axes of the normal dip-slip solutions is compatible with the NE-SW large-scale extension, whereas the orientation of the T-axes of the oblique focal mechanisms is consistent with a NNE-SSW extension. This direction of extension was already observed for the 2001 seismic sequence (Milano *et al.*, 2005), which occurred approximately 20 km towards the NE from the epicentral area of the 2010 swarm (Fig. 8). The different kinematics of the focal mechanisms suggest that this swarm

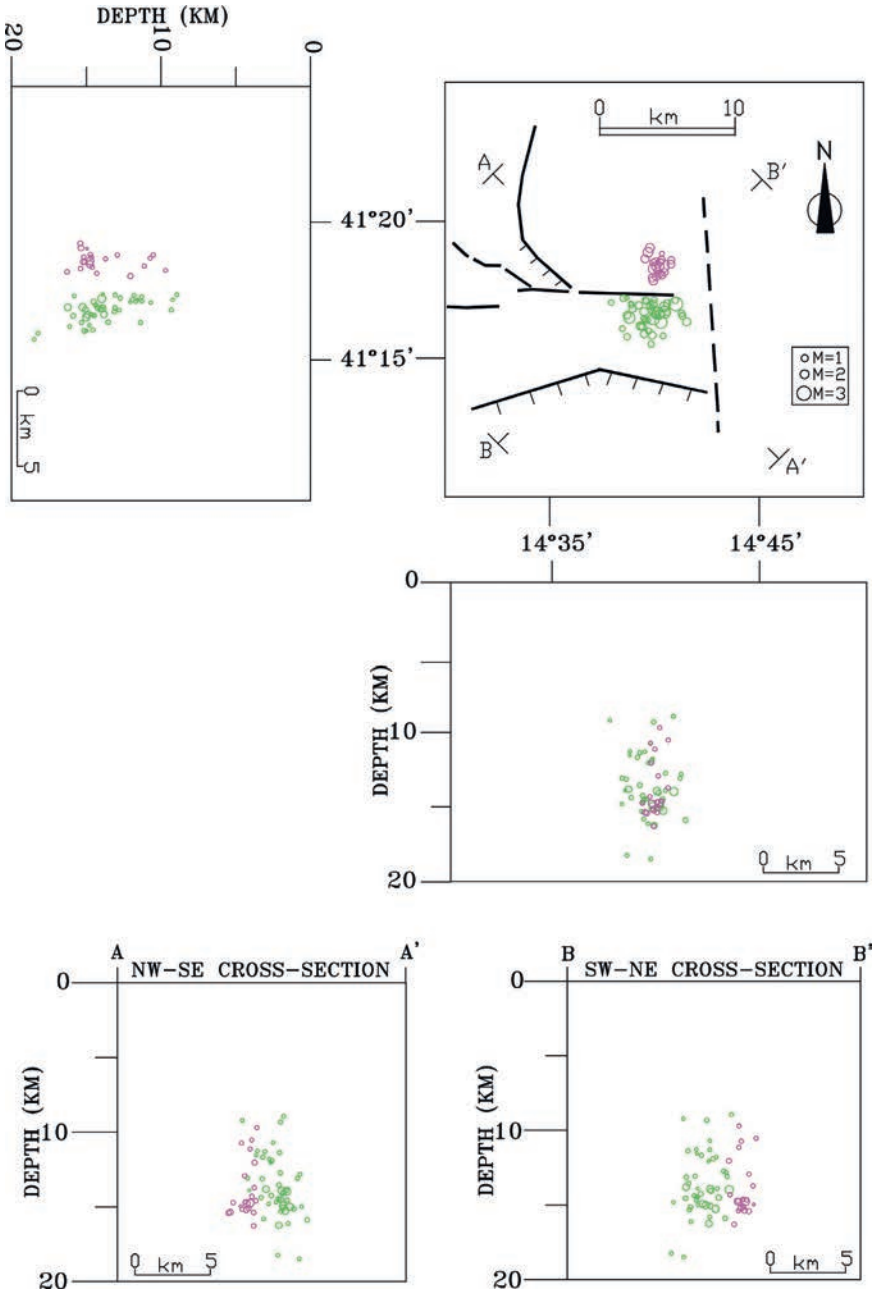

Fig. 6 - Epicentral distribution of the seismic swarms localised near the south-eastern edge of the MM and N-S, W-E, NW-SE, and NE-SW hypocentral distributions. Green circles and magenta circles denote the events belonging to the 2014 and 2018 seismic swarms, respectively.

occurred in an area characterised by structural heterogeneity, reflecting the presence of small structural lineaments with different orientations mapped at the surface (Figs. 2 and 4). The sub-horizontal T-axes of the focal mechanisms of the westernmost cluster of the 2020 swarm aligned along the NE-SW direction, whereas those of the main cluster aligned along the E-W direction. The epicentral distribution, the focal mechanisms, and the orientation of the T-axes (Fig. 5)

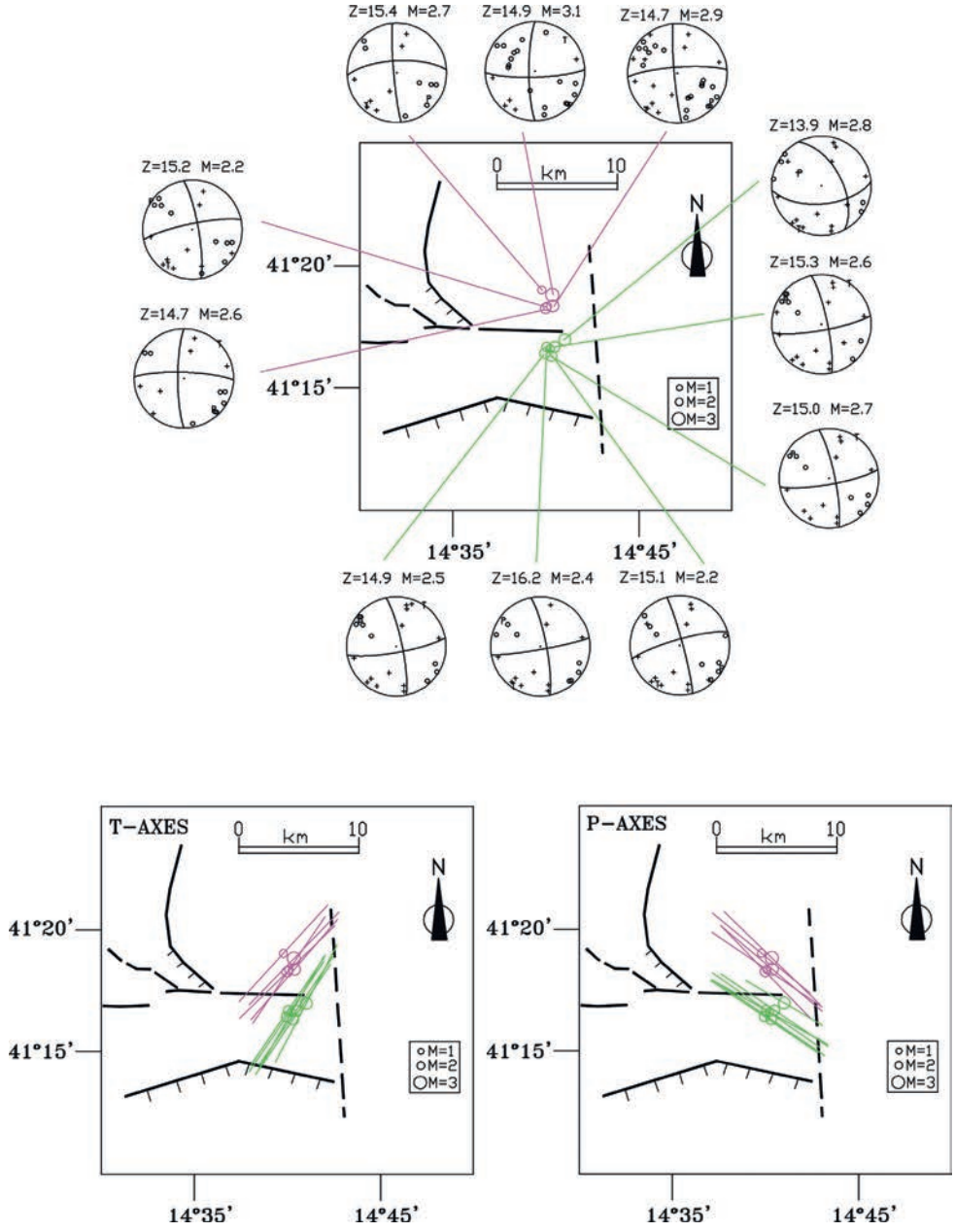

Fig. 7 - Top: fault-plane solutions of the 2014 (green) and 2018 (magenta) seismic swarms. For each focal mechanism, the depth and the magnitude of the event are reported. Bottom: surface projection of the T- (left) and P- (right) of the focal mechanisms. The length of each axis is proportional to the cosine of the plunge.

suggest that the events of the main cluster predominantly occur on a small N-S striking, normal fault segment, which moves in response to a local E-W extension.

The above considerations point to a complex strain pattern between the Venafro Mountains and the upper Volturno Valley. The release of seismic energy takes place with the occurrence of both single events and seismic swarms, and the sub-horizontal T-axes of the focal mechanisms of the swarms essentially aligned along three main directions: NE-SW, NW-SE, and E-W. A previous

study on the seismicity detected at the border between central and southern Apennines (Milano *et al.*, 2008) has shown that inside the Ortona-Roccamonfina structural lineament the seismicity, constituted by single shocks, is prevalently related to the main, NE-SW extension affecting the Apennine chain. Low magnitude seismic swarms also occur on the NE-SW to NNE-SSW striking active fault segments, moving in response to a local second-order NW-SE extension due to the chain curvature.

The results of the main cluster of the 2020 swarm suggest the presence of a local second-order E-W extension inside the Ortona-Roccamonfina, as recently proposed by Frepoli *et al.* (2017). The epicentres of the focal mechanisms, on which these authors based this assumption, are within the epicentral area of the 2020 swarm, which is located very close to the headwaters of the Volturno River. According to Hainzl *et al.* (2012), the occurrence of seismic swarms can be explained by fluid infiltration or pore pressure diffusion that reduce the normal stress level along existing fault segments. From this perspective, the main cluster of the 2020 swarm (the easternmost), as well as the events reported in Frepoli *et al.* (2017), are not due to a local E-W extension. This seismicity can be triggered by a change in the pressure of the aquifer feeding the headwaters of the Volturno River on a pre-existing ~N-S oriented blind small fault segment. In any case, we believe that these data are not sufficient to speculate on the existence of an additional E-W second-order extension within the Ortona-Roccamonfina structural lineament.

5.2. Seismicity in the south-eastern edge

The area where the 2014 and 2018 swarms are located separates the MM from the Sannio Mountains. This area is highly fractured and dissected by small structural lineaments with Apenninic, anti-Apenninic and E-W directions (Milano *et al.*, 1999). The swarms are located approximately 3 km from each other and occurred at the same depth, between 9 and 17 km. The focal mechanisms of these swarms show strike-slip solutions with ~E-W and ~N-S striking nodal planes and T- and P-axes oriented in NE-SW and NW-SE directions, respectively. The focal mechanism of a single event located between the swarms displays similar kinematics (Fig. 3). These observations suggest that the small E-W structural lineament mapped at the surface and located between the two swarms (Figs. 2 and 6) is active, extends to a depth of at least 17 km and is characterised by right-lateral strike-slip kinematics. The above suggests the presence of an active strike-slip regime in the intermediate crust near the south-eastern edge of the MM.

Recent seismological studies performed east of the MM highlighted the presence of an active strike-slip regime in the intermediate and lower crust. Adinolfi *et al.* (2015), investigating a low-magnitude sequence (M_{LMAX} = 4.1) that occurred in September 2012 about 20 km from the south-eastern edge of the MM (Fig. 8), speculated on the existence of a roughly E-W striking fault plane with right-lateral strike-slip kinematics, seated at mid-crustal depths (10-20 km). Vannoli *et al.* (2016), performing a comprehensive review of the first event of the 1962 sequence begun near the city of Benevento (Ariano Irpino earthquake of 21 August 1962, M_W = 6.1; Fig. 8), suggest that the event nucleated along an E-W striking fault system. This fault system is responsible for the southernmost event of the 1456 sequence, for a smaller, but instrumentally documented, event that occurred on 6 May 1971 (M_W = 5.0), and for the September 2012 sequence investigated by Adinolfi *et al.* (2015). De Matteo *et al.* (2018) found further evidence of strike-slip kinematics in the intermediate crust. These authors studied the seismicity at the border, between the Sannio and Irpinia regions, and suggested the co-existence of different tectonic styles at distinct crustal depths. In the upper crust, NW-SE striking normal faults prevail, whereas strike-slip faults prevail in the intermediate and lower crust. Above latitude 41° 20’ N, they found a clear prevalence

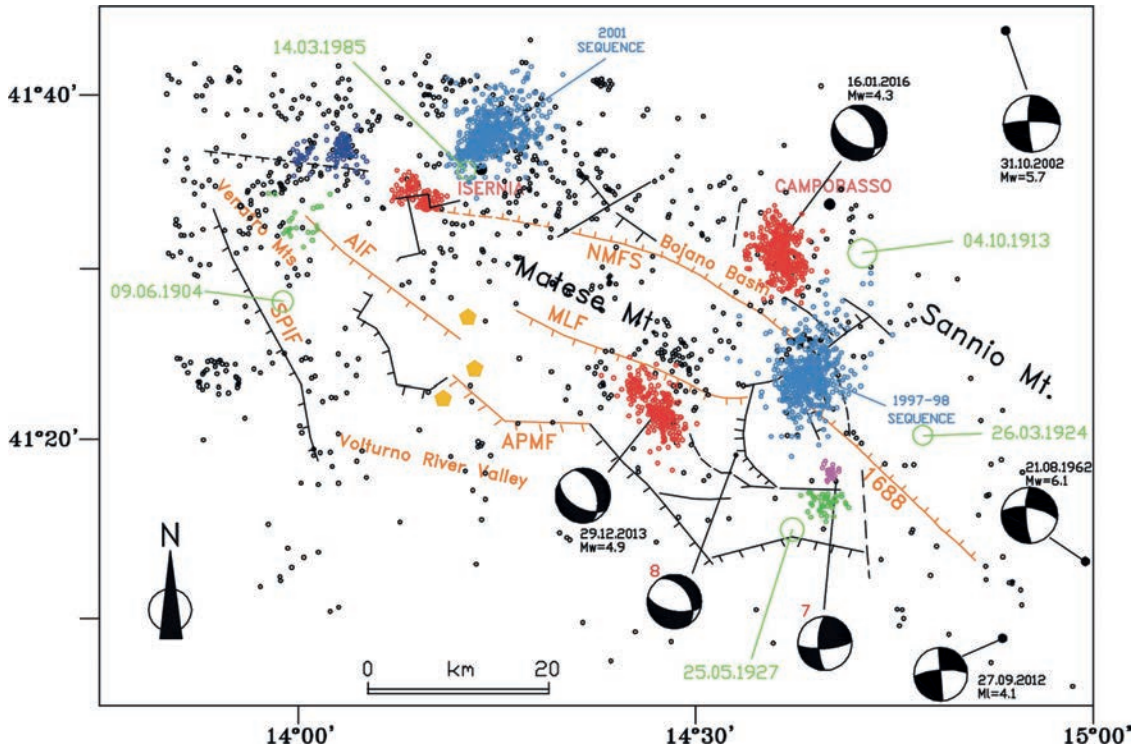

Fig. 8 - Epicentral distribution of seismicity located in the MM since 1997 [data from Milano *et al.* (2008), Ferranti *et al.* (2015), Milano (2016), and present study]. The yellow diamonds indicate the gas vents located near the AIF and the APMF. The focal mechanisms are related to: Sannio-Irpinia earthquake [21 August 1962: Vannoli *et al.* (2016)], main event of the Molise earthquake (31 October 2002, see www.ingv.it/seismoglo/RCMT), Matese earthquake [29 December 2013: Ferranti *et al.* (2015)], main event of the 2012 swarm [27 September 2012: Adinolfi *et al.* (2015)], main event of the 2016 swarm [16 January 2016: Milano (2016)]. Focal mechanisms 7 and 8 are relative to the single events located in the south-eastern edge of the MM (see Fig. 3). The events with $4.0 \leq M \leq 5.0$ (light green circles), which occurred in the area since 1900, are also reported (Rovida *et al.*, 2022).

of right lateral strike-slip kinematics along the E-W striking sub-vertical fault planes. Below latitude 41° N they noted that, according to Adinolfi *et al.* (2015), the background seismicity was closely linked to the major fault segments, activated during the M_S = 6.9 1980 earthquake, characterised by NE dipping, NW-SE striking normal faults moving in response to the NE-SW large-scale extensional regime (see also Adinolfi *et al.*, 2019, 2022).

To the west of the area, where the 2014 and 2018 swarms are located, there is no seismological evidence of a strike-slip regime. The 1997-1998 seismic sequence is located about 15 km away in the NW direction from the epicentral area of the swarms (Fig. 8). The epicentral distribution and the inversion of the focal mechanisms of this sequence suggested that it nucleated along a NNE-SSW oriented normal fault segment (Milano *et al.*, 2002). The 2013-2014 sequence, located about 20 km to the west (Fig. 8), developed on a SW dipping, a ~NW-SE oriented normal fault (Ferranti *et al.*, 2015). The 2016 sequence, located in the Bojano basin (Fig. 8), developed on a NE dipping, ~NNW-SSE oriented small fault segment (Milano, 2016; Moretti *et al.*, 2017; Trionfera *et al.*, 2020).

Strike-slip kinematics characterises the easternmost sector of the central-southern Apennines as is well attested by the 1990-1991 Potenza (M_W = 5.7) and 2002 Molise (M_W = 5.7) seismic sequences. The Potenza sequence, located about 120 km towards SE from the MM,

originated on an E-W striking right lateral strike-slip fault at the footwall of the easternmost Apennines thrust system, within the Apulian foreland crust. Hypocentres were concentrated in the middle crust between 15 and 25 km within the crystalline basement (Boncio *et al.*, 2007; Di Luccio *et al.*, 2005). The Molise sequence, located about 50 km towards NNE from the MM, originated along an E-W oriented right lateral strike-slip fault below the bottom of the carbonate sedimentary cover, within the Apulian foreland middle crust (Chiarabba *et al.*, 2005; Di Luccio *et al.*, 2005). These sequences have been interpreted as the deep seismogenic expression of active right-lateral strike-slip faults that dissect the Apulian foreland (Di Bucci and Mazzoli, 2003; Valensise *et al.*, 2004; Di Luccio *et al.*, 2005; Di Bucci *et al.*, 2006; Boncio *et al.*, 2007; De Matteis *et al.*, 2012).

With the above considerations, we assume that the area where the 2014 and 2018 swarms occurred could represent the westernmost expression of the active strike-slip regime of the Apulian foreland. This strike-slip regime acts between latitude 41° 20' N, assumed to be the border between the Sannio and Irpinia regions (De Matteo *et al.*, 2018), and latitude 41° 45' N, the location of the well-known Molise-Mattinata-Gondola major shear zone (e.g. Vannoli *et al.*, 2021) on which the 2002 Molise earthquake is located. The area that separates the Matese from the Sannio Mountains could also mark the passage to the NE-SW oriented normal faults that characterise the inner Apennine chain.

5.3. Seismicity in the inner and along the southern side

The inner and axial portion of the Apennine chain is affected by degassing of massive amounts of CO_2 (Chiodini *et al.*, 2004; Minissale, 2004; Ventura *et al.*, 2007; Frezzotti *et al.*, 2009; Burton *et al.*, 2013). High fluid pressure at depth can play a major role in triggering earthquakes (Chiodini *et al.*, 2004), due to the reduction of normal stress levels on existing faults, and a continuous CO_2 production process facilitates the formation of over-pressurised CO_2-rich reservoirs, potentially able to trigger earthquakes at crustal depth (Chiodini *et al.*, 2020). Several CO_2-rich springs and areas of diffuse degassing through the soil are located in the MM [see Fig. 1 in Rufino *et al.* (2021)]. Ascione *et al.* (2018) revealed an anomalously high flux of CO_2 concentrated in gas vents located along the fault segments of the major crustal structures of the southern side of the MM. This very high gas emission is the result of both the presence of a dense network of active fault stands, which provide efficient pathways for fluid flow towards the surface, and the dramatically reduced thickness of the clay-rich melange zone acting elsewhere in the southern Apennines as a top seal overlying the buried Apulian platform carbonates (Ascione *et al.*, 2018).

The gas vents are located between the south-eastern area of the AIF and the south-western area of the APMF (yellow diamonds in Fig. 8). The seismic activity along these faults is very rare also considering the seismicity since 1997 (Fig. 8). We believe that a continuous and constant degassing from gas vents and through a dense network of fault stands, observed by Ascione *et al.* (2018), may not favour the increment of pore pressure on a fault or the formation of over-pressurised CO_2-rich reservoirs in the crust able to trigger earthquakes. Under such condition, only tectonic stress and the lithostatic pressure can act in depth on a pre-existing fault. The very high flux of CO_2 and the lack of seismicity in the area where the gas vents are located suggest the anti-correlation between high CO_2 discharges and seismicity. However, the correlation or the anti-correlation between the rates of CO_2 discharge-seismicity rate needs the knowledge of a long-time series of CO_2 discharges of a seismogenic area, which are currently not collected for the MM. Continuous monitoring of the area allows the acquisition of this information.

The epicentral distribution since 1997 shows that the seismicity occurred prevalently in the

SE of the MM, as evidenced by the 1997-1998, 2013-2014, and 2016 sequences, and in the NW, as evidenced by the 2001 sequence and 2010 swarm (Fig. 8). Along the southern side, seismicity detected is very rare and there is no information on the occurrence of seismic events with $4.0 \leq M \leq 5.0$ since 1900 (see Rovida *et al.*, 2022). This rare seismicity does not imply that the major crustal structures that border the southern side of the MM are not active; the lack of seismicity may be due to the high gas emission along the dense network of fault stands (Ascione *et al.*, 2018). The seismic activity in the inner area, between the AIF, APMF, and MLF, is also very rare and attributable to high gas emission. Tomographic studies already evidenced the low seismicity in the central zone of the MM (Bisio *et al.*, 2004). The lack of seismicity was related to the presence of a crustal volume characterised by high *Vp* beneath the central area of the MM, considering that the presence of high *Vp* regions is interpreted as high-strength materials able to store large stress (Foxall *et al.*, 1993; Zhao and Negishi, 1998). In any case, further geological and geophysical investigations are required to verify the hypothesis on the anti-correlation between the high CO_2 emissions and very rare seismicity.

6. Concluding remarks

We investigated the 2009-2020 background seismicity of the Matese Massif in order to provide new constraints on the seismotectonics of its southern side. The results, discussed with the results of the recent geophysical and geological investigations, further highlight the structural complexity of the massif. The main results of this study are summarised below.

The 2009-2020 background seismicity occurred mainly through low-magnitude seismic swarms, located at the NW and SE edges of the MM, and single shocks that occurred sparsely without any preferential alignment. The focal mechanisms of the single events localised in the depression of the Volturno River valley, that borders the western and north-western sides of the MM, suggest that the seismicity occurs on the SW dipping, NW-SE oriented fault segments, in accordance with the kinematics of the normal faults mapped at the surface. The seismic swarms located between the NW tip of the AIF and the NW tip of the NMFS occurred on small fault segments striking in different directions. This seismicity is mainly associated with the large-scale NE-SW extension that characterises the Apennine chain, but it is also associated with the NW-SE, second order extension found in the Ortona-Roccamonfina lineament and is caused by the curvature of the chain. Fluid infiltration or pore pressure diffusion could trigger the seismic swarms, as assumed for the 2020 swarm.

The focal mechanisms of two low-magnitude seismic swarms and the focal mechanism of a single shock located near the south-eastern edge of the MM suggest the existence, never previously observed in this area, of an active E-W striking fault segment with dextral strike-slip kinematics in the intermediate crust. To the west of this area, which is the inner part of the massif, there is no seismological evidence of strike-slip kinematics, whereas such evidence is found to the east in the intermediate crust. The morphological depression that separates the MM from the Sannio Mountains could represent the westernmost expression of the active strike-slip regime that characterises the Apulian foreland between latitude 41° 20’ N and 41° 45’ N. This area also marks the passage, towards the west, to the NE-SW oriented normal faults that characterise the inner Apennine chain. The existence of an active E-W fault segment, characterised by strike-slip kinematics near the south-eastern edge of the MM, could also furnish a new stimulus towards redefining the 1688 relevant seismogenic structure, its NW tip being located in the morphological depression that separates the MM from the Sannio Mountains.

The epicentral distribution since 1997 shows that the seismic activity concentrates mainly in the eastern sector of the MM, as evidenced by the 2013-2014 and 2016 sequences, and by low-magnitude single shocks ($M \leq 2.0$) located between the epicentral areas of these sequences. Further east, the 1997-1998 sequence and the 2014 and 2018 swarms are located in the depression dividing the MM from the Sannio Mountains. In the area between the AIF, the APMF and MLF, and along the southern side, seismicity detected is very scarce. This scarce seismicity may be due to the anomalously high-flux of CO_2 concentrated in gas vents located near these faults. A dense network of fault strands, belonging to major crustal structures of the southern side, facilitates gas emission. To corroborate the hypothesis of high CO_2 emission - rare seismicity detected, knowledge of a long-time series of CO_2 discharges is required and, at present, this has not been achieved for the MM.

Considering the time elapsed since the last destructive earthquake (1349), the possible sources of the poorly known 346 and 1293 earthquakes (indicating that they most likely occurred along the southern side), the scarce instrumental seismicity detected in the last 25 years in the central and along the southern side (probably also due to high gas emission), and the lack of earthquakes with $4.0 \leq M \leq 5.0$ since 1900, lead to speculating that the south-western side of the MM may be affected by large earthquakes in the future. This hypothesis would imply the possible redefinition of the seismic hazard of the area. We retain that further independent geological and geophysical investigations, in particular, geochemical monitoring to collect a long-time series of CO_2 discharges in the whole area, are required. We hope that the results of this study can also be a stimulus to target multidisciplinary investigations to further deepen the knowledge of the MM and the areas bordering it.

Acknowledgments. We thank Guido Maria Adinolfi and an anonymous reviewer for their critical reviews and useful comments on the manuscript. We also thank the Editor, Dario Slejko, and we appreciated the assistance of the Associate Editor, Stefano Parolai. We are grateful to Danilo Galluzzo for his help in managing the seismic test station installed in the upper Volturno Valley.

REFERENCES

Adinolfi G.M., De Matteis R., Orefice A., Festa G., Zollo A., De Nardis R. and Lavecchia G.; 2015: *The September 27, 2012, ML 4.1, Benevento earthquake: a case of strike-slip faulting in southern Apennines (Italy)*. Tectonophys., 660, 35-46, doi: 10.1016/j.tecto.2015.06.036.

Adinolfi G.M., Cesca S., Picozzi M., Heimann S. and Zollo A.; 2019: *Detection of weak seismic sequences based on arrival time coherence and empiric network detectability: an application at a near fault observatory*. Geophys. J. Int., 218, 2054-2065.

Adinolfi G.M., De Matteis R., De Nardis R. and Zollo A.; 2022: *A functional tool to explore the reliability of micro-earthquake focal mechanism solutions for seismotectonic purposes.* Solid Earth, 13, 65-83, doi: 10.5194/se-13-65-2022.

Ascione A., Ciotoli G., Bigi S., Buscher J., Mazzoli S., Ruggiero L., Sciarra A., Tartarello M.C. and Valente E.; 2018: *Assessing mantle versus crustal sources for nonvolcanic degassing along fault zones in the actively extending southern Apennines mountain belt (Italy).* Geol. Soc. Am. Bull., 130, 1697-1722, doi: 10.1130/B31869.1.

Bisio L., Di Giovambattista R., Milano G. and Chiarabba C.; 2004: *Three-dimensional earthquake locations and upper crustal structure of the Sannio-Matese region (southern Italy).* Tectonophys., 385, 121-136.

Boncio P., Mancini T., Lavecchia G. and Selvaggi G.; 2007: *Seismotectonics of strike-slip earthquakes within the deep crust of southern Italy: geometry, kinematics, stress field and crustal rheology of the Potenza 1990-1991 seismic sequences (Mmax 5.7).* Tectonophys., 445, 281-300.

Boncio P., Dichiarante A.M., Auciello E., Saroli M. and Stoppa F.; 2016: *Normal faulting along the western side of the Matese Mountains: implications for active tectonics in the central Apennines (Italy).* J. Struct. Geol., 82, 16-36, doi: 10.1016/j.jsg.2015.10.005.

Boncio P., Auciello E., Amato V., Aucelli P., Petrosino P., Tangari A.C., and Jicha B.R.; 2022: *Late Quaternary faulting in the southern Matese (Italy): implications for earthquake potential and slip rate variability in the southern Apennines*. Solid Earth, 13, 553-582, doi: 10.5194/se-13-553-2022.

Burton M.R., Sawyer G.M. and Granieri D.; 2013: *Deep carbon emissions from volcanoes.* Rev. Mineral. Geochem., 75, 323-354, doi: 10.2138/rmg.2013.75.11.

Calabrò R.A., Corrado S., Di Bucci D., Robustini P. and Tornaghi M.; 2003: *Thin-skinned vs. tick-skinned tectonics in the Matese Massif, central-southern Apennines (Italy).* Tectonophys., 377, 269-297, doi: 10.1016/j.tecto.2003.09.010.

Chiarabba C. and Amato A.; 1997: *Upper crustal structure of the Benevento area (southern Italy): fault heterogeneities and potential for large earthquakes*. Geophys. J. Int., 130, 229-239.

Chiarabba C., De Gori P., Chiaraluce L., Bordoni P., Cattaneo M., De Martin M., Frepoli A., Michelini A., Monachesi A., Moretti M., Augliera G.P., D'Alema E., Frapiccini M., Gassi A., Marzorati S., Di Bartolomeo P., Gentile S., Govoni A., Lovisa L., Romanelli M., Ferretti G., Pasta M., Spallarossa D. and Zunino E.; 2005: *Mainshocks and aftershocks of the 2002 Molise seismic sequence, southern Italy*. J. Seismol., 9, 487-494.

Chiodini G., Cardellini C., Amato A., Boschi E., Caliro S., Frondini F. and Ventura G.; 2004: *Carbon dioxide Earth degassing and seismogenesis in central and southern Italy*. Geophys. Res. Lett., 31, L07615, 1-4, doi: 10.1029/2004GL019480.

Chiodini G., Cardellini C., Di Luccio F., Selva J., Frondini F., Caliro S., Rosiello A., Beduini G. and Ventura G.; 2020: *Correlation between tectonic CO2 Earth degassing and seismicity is revealed by a 10-year record in the Apennines, Italy*. Sci. Adv., 6, 1-7, doi: 10.1126/sciadv.abc2938.

CNR-PFG; 1983: *Neotectonic map of Italy, scale 1:500,000, Sheet 4.* Consiglio Nazionale delle Ricerche, Progetto Finalizzato Geodinamica, Sottoprogetto Neotettonica, Roma, Italy.

Cowie P.A., Phillips R.J., Roberts G.P., McCaffrey K., Zijerveld L.J.J., Gregory L.C., Faure Walker J., Wedmore L.N.J., Dunai T.J., Binnie S.A., Freeman S.P.H.T., Wilcken K., Shanks R.P., Huismans R.S., Papanikolaou I., Michetti A.M. and Wilkinson M.; 2017: *Orogen-scale uplift in the central Italian Apennines drives episodic behaviour of earthquake faults*. Sci. Rep., 7, 44858, doi: 10.1038/srep44858.

De Matteis R., Matrullo E., Rivera L., Stabile T.A., Pasquale G. and Zollo A.; 2012: *Fault delineation and regional stress direction from the analysis of background microseismicity in the southern Apennines, Italy.* Bull. Seismol. Soc. Am., 102, 1899-1907, doi: 10.1785/0120110225.

De Matteo A., Massa B., Milano G. and D'Auria L.; 2018: *A transitional volume beneath the Sannio-Irpinia border region (southern Apennines): different tectonic styles at different depths.* Tectonophys., 723, 14-26, doi: 10.1016/j.tecto.2017.12.005.

Di Bucci D. and Mazzoli S.; 2003: *The October-November 2002 Molise seismic sequence (southern Italy): an expression of Adria intraplate deformation.* J. Geol. Soc., 160, 503-506, doi: 10.1144/0016-764902-152.

Di Bucci D., Massa B., Tornaghi M. and Zuppetta A.; 2005a: *Structural setting of the 1688 Sannio earthquake epicentral area (southern Italy) from surface and subsurface data.* J. Geodyn., 40, 294-315.

Di Bucci D., Naso G., Corrado S. and Villa I.M.; 2005b: *Growth, interaction and seismogenic potential of coupled active normal faults (Isernia basin, central-southern Italy). T*erra Nova, 17, 44-55.

Di Bucci D., Ravaglia A., Seno S., Toscani G., Fracassi U. and Valensise G.; 2006: *Seismotectonics of the southern Apennines and Adriatic foreland: insights on active regional E-W shear zones from analogue modeling*. Tectonics, 25, 1-21, doi: 10.1029/2005TC001898.

Di Luccio F., Piscini A., Pino N.A. and Ventura G.; 2005: *Reactivation of deep faults beneath southern Apennines: evidence from the 1990-1991 Potenza seismic sequences*. Terra Nova, 17, 586-590, doi: 10.1111/j.1365-3121.2005.00653.x.

Di Luccio F., Chiodini G., Caliro S., Cardellini C., Convertito V., Pino N.A., Tolomei C. and Ventura G.; 2018: *Seismic signature of active intrusions in mountain chains*. Sci. Adv., 4, 1-9, doi: 10.1126/sciadv.1701825.

DISS Working Group; 2021: *Database of Individual Seismogenic Sources (DISS), version 3.3.0: a compilation of potential sources for earthquakes larger than M 5.5 in Italy and surrounding areas*. Istituto Nazionale di Geofisica e Vulcanologia (INGV), doi: 10.13127/diss3.3.0.

Esposito A., Galvani A., Sepe V., Atzori S., Brandi G., Cubellis E., De Martino P., Dolce M., Massucci A., Obrizzo F., Pietrantonio G., Riguzzi F. and Tammaro U.; 2020: *Concurrent deformation processes in the Matese Massif area (central - southern Apennines, Italy)*. Tectonophys., 774, 228234, doi: 10.1016/j.tecto.2019.228234.

Ferranti L.; 1997: *Tettonica tardo Pliocenica - Quaternaria dei Monti del Matese (Appennino Meridionale): raccorciamenti tardivi e distensione "neotettonica".* Il Quaternario, 10, 501-504.

Ferranti L., Milano G., Burrato P., Palano M. and Cannavo F.; 2015: *The seismogenic structure of the 2013-2014 Matese seismic sequence, southern Italy: implication for the geometry of the Apennines active extensional belt*. Geophys. J. Int., 201, 823-837, doi: 10.1093/gji/ggv053.

Foxall W., Michelini A. and Mc Evilly T.V.; 1993: *Earthquake travel time tomography of southern Santa Cruz Mountains: control of fault heterogeneity of the San Andrea Fault zone*. J. Geophys. Res., 98, 17691-17710.

Fracassi U. and Valensise G.; 2007: *Unveiling the sources of the catastrophic 1456 multiple earthquake: hints to an unexplored tectonic mechanism in southern Italy*. Bull. Seismol. Soc. Am., 97, 725-748.

Frepoli A., Cimini G.B., De Gori P., De Luca G., Marchesetti A., Monna S., Montuosi C. and Pagliuca N.M.; 2017: *Seismic sequences and swarms in the Latium - Abruzzo - Molise Apennines (central Italy): new observations and analysis from dense monitoring of the recent activity*. Tectonophys., 712-713, 312-329, doi: 10.1016/j.tecto.2017.05.026.

Frezzotti M.L., Peccerillo A. and Panza G.; 2009: *Carbonate metasomatism and CO2 lithosphere - asthenosphere degassing beneath the western Mediterranean: an integrated model arising from petrological and geophysical data*. Chem. Geol., 262, 108-120.

Galli P. and Galadini F.; 2003: *Disruptive earthquakes revealed by faulted archaeological relics in Samnium (Molise, southern Italy).* Geophys. Res. Lett., 30, 1266, doi: 10.1029/2002GL016456.

Galli P. and Naso J.A.; 2009: *Unmasking the 1349 earthquake source (southern Italy): palaeoseismological and archaeoseismological indications from the Aquae Iuliae Fault.* J. Struct. Geol., 31, 128-149.

Galli P., Galadini F. and Capini S.; 2002: *Analisi archeosismologiche nel santuario di Ercole di Campochiaro (Matese). Evidenze di un terremoto distruttivo sconosciuto ed implicazioni sismotettoniche*. Il Quaternario (Ital. J. Quat. Sci.), 15, 151-163.

Giuliani R., D'Agostino N., D'Anastasio E., Mattone M., Bonci L., Calcaterra S., Gambino P. and Merli K.; 2009: *Active crustal extension and strain accumulation from GPS data in the Molise region (centralsouthern Apennines, Italy).* Boll. Geof. Teor. Appl., 50, 145-156.

Guidoboni E., Ferrari G., Mariotti D., Comastri A., Tarabusi G. and Valensise G.; 2007: *CFTI4Med, Catalogue of Strong Earthquakes in Italy (461 B.C.-1997) and Mediterranean Area (760 B.C.-1500)*. INGV-SGA, Roma-Bologna, Italy, <storing.ingv.it/cfti4med>.

Hainzl S., Fischer T. and Dahm T.; 2012: *Seismicity-based estimation of the driving fluid pressure in the case of swarm activity in western Bohemia*. Geophys. J. Int., 191, 271-281.

Iannaccone G., Improta L., Capuano P., Zollo A., Biella G., De Franco R., Deschamps A., Cocco M., Mirabile L. and Romeo R.; 1998: *A P-wave velocity model of upper crust of Sannio region (southern Apennines, Italy)*. Ann. Geofis., 41, 567-582.

Improta L., Iannaccone G., Capuano P., Zollo A. and Scandone P.; 2000: *Inferences on the upper crustal structure of southern Appenines (Italy) from seismic refraction investigations and subsurface data.* Tectonophys., 317, 273-297.

Klein F.W.; 2002: *User's guide to HYPOINVERSE-2000, a Fortran program to solve for earthquake locations and magnitudes, version 4/2002*. U.S. Geol. Surv., Open file report 02-171, Menlo Park, CA, USA, 123 pp.

Milano G.; 2014: *Seismological investigation of the 2013-2014 seismic sequence of the Matese Massif (southern Apennines, Italy).* In: Atti 33° Convegno Nazionale, Gruppo Nazionale Geofisica Terra Solida, Bologna, Italy, pp. 79-84.

Milano G.; 2016: *Seismological investigation of the 2016 low-magnitude seismic sequence near Baranello (Sannio-Matese area, southern Apennines - Italy): first results.* In: Atti 35° Convegno Nazionale, Gruppo Nazionale Geofisica Terra Solida, Lecce, Italy, pp. 149-151.

Milano G., Di Giovambattista R. and Alessio G.; 1999: *Earthquake swarms in the southern Apennines chain (Italy): the 1997 seismic sequence in the Sannio-Matese Mountains.* Tectonophys., 306, 57-78.

Milano G., Ventura G. and Di Giovambattista R.; 2002: *Seismic evidence of longitudinal extension in the southern Apennines chain (Italy): the 1997-1998 Sannio-Matese seismic sequence.* Geophys. Res. Lett*.,* 29, 65-1-65-4, doi: 10.1029/2002GL015188.

Milano G., Di Giovambattista R. and Ventura G.; 2005: *The 2001 seismic activity near Isernia (Italy): implications for the seismotectonics of the central-southern Apennines.* Tectonophys*.,* 401, 167-178.

Milano G., Di Giovambattista R. and Ventura G.; 2008: *Seismic activity in the transition zone between southern and central Apennines (Italy): evidences of longitudinal extension inside the Ortona-Roccamonfina tectonic line.* Tectonophys., 457, 102-110.

Minissale A.; 2004: *Origin, transport and discharge of CO2 in central Italy.* Earth Sci. Rev., 66, 89-141.

Moretti M., Margheriti L., Basili A., Baccheschi P., Villani F., Cecere G., D'Ambrosio C., Di Stefano R., Falco L., Memmolo A., De Luca G., Migliari F., Minichiello F. and Scognamiglio L.; 2017: *Il terremoto a Campobasso del 16 gennaio 2016. L'evento di M_w 4.3 e la sequenza sismica associata*. Quaderni di Geofisica, 140, 1-29, doi: 10.13127.

Porfido S., Esposito E., Vittori E., Tranfaglia G., Michetti A.M., Blumetti M., Ferreli L., Guerrieri L. and Serva L.; 2002: *Areal distribution of ground effects induced by strong earthquakes in the southern Apennines (Italy).* Surv. Geophys., 23, 529-562.

Reasenberg P. and Oppenheimer D.; 1985: *FPFIT, FPPLOT and FPPAGE: Fortran computer programs for calculating and displaying earthquake fault plane solutions.* U.S. Geol. Surv., Open file report 85-739, Menlo Park. CA, USA, 109 pp., doi: 10.3133/ofr85739.

Rovida A., Locati M., Camassi R., Lolli B., Gasperini P. and Antonucci A.; 2022: *Catalogo Parametrico dei Terremoti Italiani (CPTI15), versione 4.0*. Istituto Nazionale di Geofisica e Vulcanologia (INGV), Roma, Italy, doi: 10.13127/CPTI/CPTI15.4.

Rufino F., Cuoco E., Busico G., Caliro S., Maletic E.L., Avino R., Darrah T.H. and Tedesco D.; 2021: *Deep carbon degassing in the Matese Massif chain (southern Italy) inferred by geochemical and isotopic data.* Environ. Sci. Pollut. Res. Int., 28, 46614-46626, doi: 10.1007/s11356-020-11107-1.

Trionfera B., Frepoli A., De Luca G., De Gori P. and Doglioni C.; 2020: *The 2013-2018 Matese and Beneventano seismic sequences (central-southern Apennines): new constraints on the hypocentral depth determination.* Geosci., 10, 17, doi: 10.3390/geosciences10010017.

Valensise G., Pantosti D. and Basili R.; 2004: *Seismology and tectonic setting of the 2002 Molise, Italy, earthquake*. Earthquake Spectra, 20, S23-S37, doi: 10.1193/1.1756136.

Vannoli P., Bernardi F., Palombo B., Vannucci G., Console R. and Ferrari G.; 2016: *New constraints shed light on strike-slip faulting beneath the southern Apennines (Italy): the 21 August 1962 Irpinia multiple earthquake.* Tectonophys., 691, 375-384, doi: 10.1016/j.tecto.2016.10.032.

Vannoli P., Martinelli G. and Valensise G.; 2021: *The seismotectonic significance of geofluids in Italy*. Front. Earth Sci., 9, 5793901, 25 pp., doi: 10.3389/feart.2021.579390.

Ventura G., Cinti F.R., Di Luccio F. and Pino N.A.; 2007: *Mantle wedge dynamics versus crustal seismicity in the Apennines (Italy)*. Geochem. Geophys. Geosyst., 8, Q02013, doi: 10.1029/2006GC001421.

Zhao D. and Negishi H.; 1998: *The 1995 Kobe earthquake; seismic image of the source zone and its implications for the rupture nucleation.* J. Geophys. Res. Solid Earth, 103, 9967-9986, doi: 10.1029/97JB03670.

Corresponding author: Girolamo Milano
Istituto Nazionale di Geofisica e Vulcanologia
Osservatorio Vesuviano - Sezione di Napoli INGV
Via Diocleziano 328, 80124 Napoli, Italy
Phone: +39 081 6108331, e-mail: girolamo.milano@ingv.it